

## Support information

### **Simultaneous Removal of Phosphates and Dyes by Al-doped Iron Oxides Decorated MgAl Layered Double Hydroxide Nanoflakes**

Shu Cheng,<sup>a</sup> Luhua Shao,<sup>a</sup> Jianhong Ma,<sup>bc</sup> Xinnian Xia,<sup>\*a</sup> Yutang Liu,<sup>bc</sup> Zhenfei Yang,

<sup>a</sup> Cong Yang,<sup>a</sup> Sijian Li<sup>a</sup>

<sup>a</sup> *College of Chemistry and Chemical Engineering, Hunan University, Lushan South Road, Yuelu District, Changsha 410082, P. R. China*

<sup>b</sup> *College of Environmental Science and Engineering, Hunan University, Lushan South Road, Yuelu District, Changsha 410082, P. R. China*

<sup>c</sup> *Key Laboratory of Environmental Biology and Pollution Control (Hunan University), Ministry of Education, Lushan South Road, Yuelu District, Changsha 410082, P.R. China*

Corresponding author

Xinnian Xia

College of Chemistry and Chemical Engineering, Hunan University, Lushan South Road, Yuelu District, Changsha 410082, P. R. China

E-mail address: [xnxia@hnu.edu.cn](mailto:xnxia@hnu.edu.cn) (X. N Xia)

## Adsorption kinetics models

The pseudo-first-order, pseudo-second-order models were used to describe the experimental adsorption kinetic data. The mathematical equations of the pseudo-first-order model (Eq. S1), pseudo-second-order model (Eq. S2) are expressed as follows:

$$\log(q_e - q_t) = \log q_e - \frac{k_1 t}{2.303} \quad (S1)$$

$$\frac{t}{q_t} = \frac{1}{k_2 q_e^2} + \frac{t}{q_e} \quad (S2)$$

where  $k_1$  ( $\text{min}^{-1}$ ) and  $k_2$  ( $\text{g mg}^{-1} \text{ min}^{-1}$ ) are the pseudo-first order and pseudo-second-order rate constants, respectively.

## Adsorption isotherms and thermodynamics

The linear forms of Langmuir (Eq. S3), Freundlich (Eq. S4) and Langmuir-Freundlich (Eq. S5) isotherm models are respectively expressed as follows.

$$q_e = \frac{q_{\max} K_L C_e}{1 + K_L C_e} \quad (S3)$$

$$q_e = K_F C_e^{1/n_F} \quad (S4)$$

$$q_e = \frac{K_{LF} C_e^{1/n}}{1 + a_{LF} C_e^{1/n}} \quad (S5)$$

where  $q_e$  ( $\text{mg/g}$ ) is the equilibrium adsorption capacity,  $q_{\max}$  ( $\text{mg/g}$ ) is the maximum adsorption capacity,  $K_L$  ( $\text{L/mg}$ ),  $K_F$  ( $\text{mg}^{1-1/n} \text{L}^{1/n} \text{g}^{-1}$ ),  $K_{LF}$  ( $\text{mg}^{1-1/n_F} \text{L}^{1/n_F} \text{g}^{-1}$ ) and  $a_{LF}$  ( $\text{mg}^{-1/n} \text{L}^{1/n}$ ) are the corresponding adsorption equilibrium constants,  $n_F$  represents the degree of adsorption and  $n$  is heterogeneity parameter.

The values of  $\Delta G^0$ ,  $\Delta H^0$  and  $\Delta S^0$  can be calculated from the following equation(Eq. S6, S7).

$$\Delta G^0 = -RT \ln K^0 \quad (S6)$$

$$\ln K^0 = \frac{\Delta S^0}{R} - \frac{\Delta H^0}{RT} \quad (S7)$$

where  $R$  ( $8.314 \text{ J mol}^{-1} \text{ K}^{-1}$ ) is the ideal gas constant,  $T$  is the temperature in kelvin.  $K^0$  is the equilibrium constant, which is calculated from plotting of  $\ln K_d$  vs  $C_e$ , at the  $C_e$  is value of zero, the intercept is  $\ln K^0$ .

### **Simultaneous removal studies**

The values of removal capacities ratio( $R_q$ ) can be calculated as follows(Eq. S8):

$$R_q = q_{b,i} / q_{m,i} \quad (S8)$$

where  $q_{b,i}$  is the removal capacities of pollutant i in the binary system and  $q_{m,i}$  is the removal capacities of pollutant i in the mono-component system under the same conditions. It has been reported that (i) if  $R_q > 1$ , the existence of pollutant j can promote the removal efficiency of pollutant i; (ii) if  $R_q = 1$ , the existence of pollutant j has no effect on the removal efficiency of pollutant i; (iii) if  $R_q < 1$ , the existence of pollutant j can inhibit the removal efficiency of pollutant i.

### **Desorption efficiencies**

The desorption efficiency ( $R_D$ ) can be calculated from the equation as follows(Eq. S9):

$$R_D(\%) = \frac{C_d \times V_d}{q_e \times m} \times 100 \quad (S9)$$

where  $C_d$  is the desorbed phosphate concentration (mg P/L),  $V_d$  is the volume of solution (L) during desorption processes,  $q_e$  is the adsorbed amount before desorption (mg P/g) and  $m$  is the mass of the adsorbent (g).

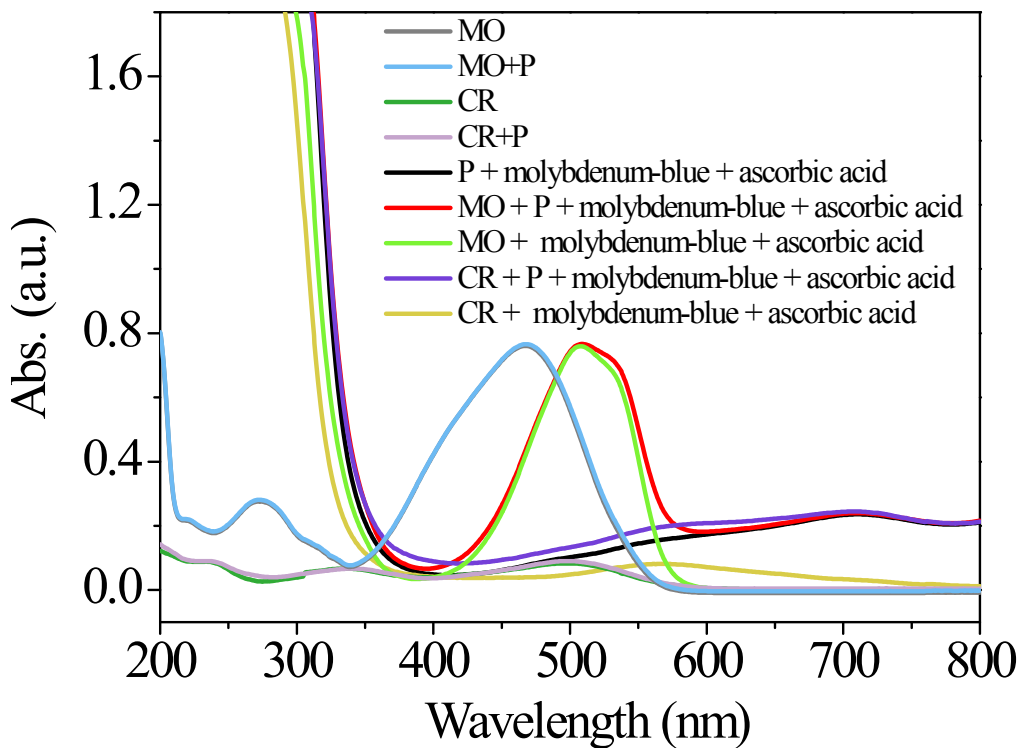


**Fig.S1.** UV-Vis spectra of the individual and mixed solution before and after adding molybdenum-blue and ascorbic acid,  $C_p$  initial = 10 mg/L,  $C_{MO}$  initial =  $C_{CR}$  initial = 200 mg/L, dilution before UV test.

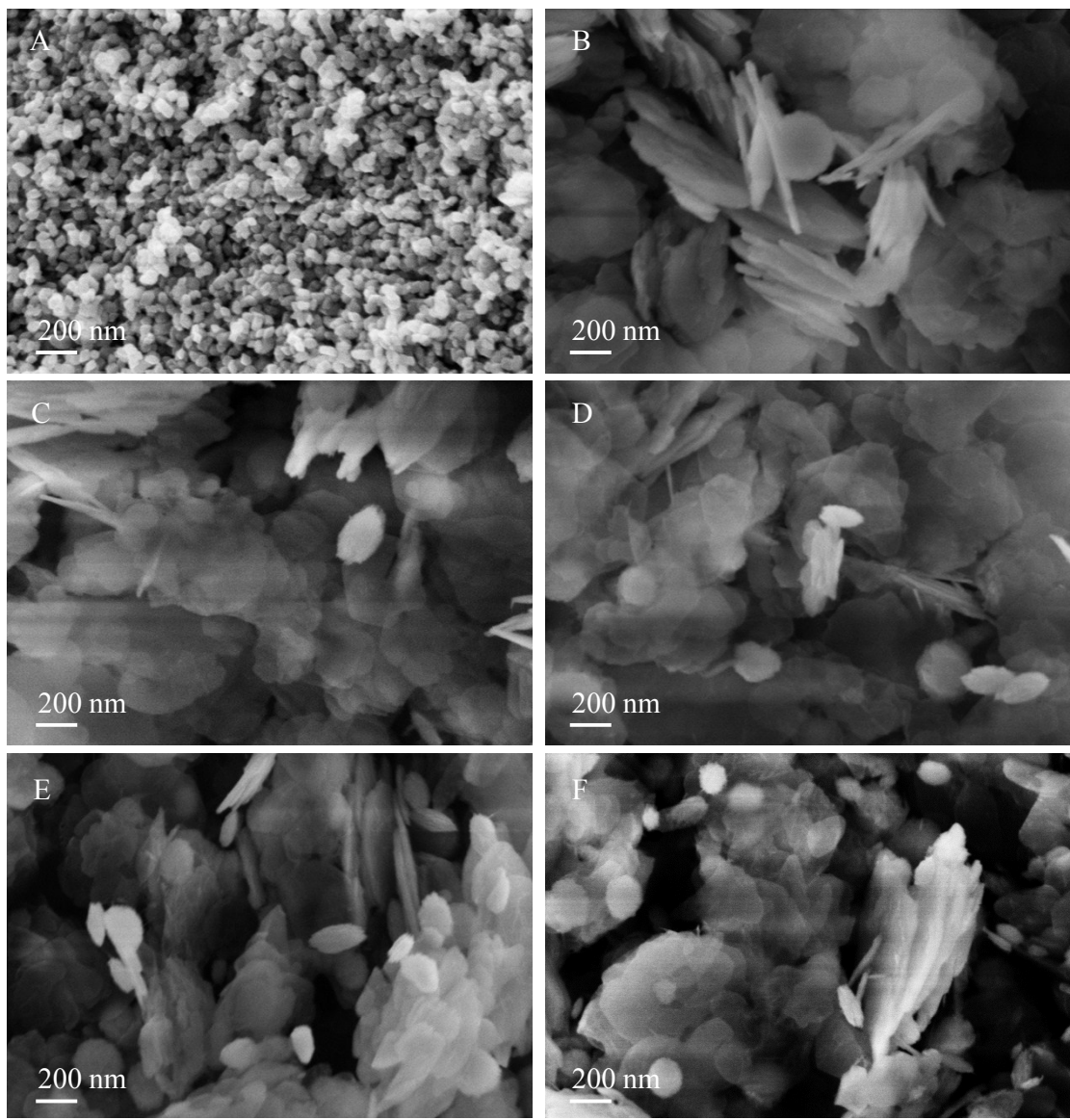


**Fig. S2.** SEM images of free  $\text{Al}-\text{Fe}_2\text{O}_3$  (A),  $0.3\text{Al}-\text{Fe}_2\text{O}_3/\text{LDH}$  (B),  $0.5\text{Al}-\text{Fe}_2\text{O}_3/\text{LDH}$  (C),  $0.8\text{Al}-\text{Fe}_2\text{O}_3/\text{LDH}$  (D),  $1.5\text{Al}-\text{Fe}_2\text{O}_3/\text{LDH}$  (E) and  $2\text{Al}-\text{Fe}_2\text{O}_3/\text{LDH}$  (F)

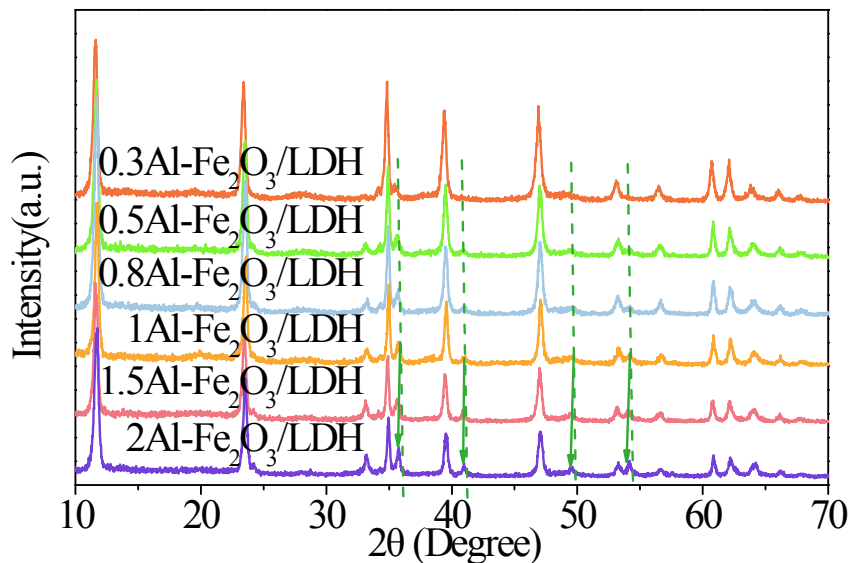


**Fig.S3.** XRD patterns of Al-Fe<sub>2</sub>O<sub>3</sub>/LDH assemblies.

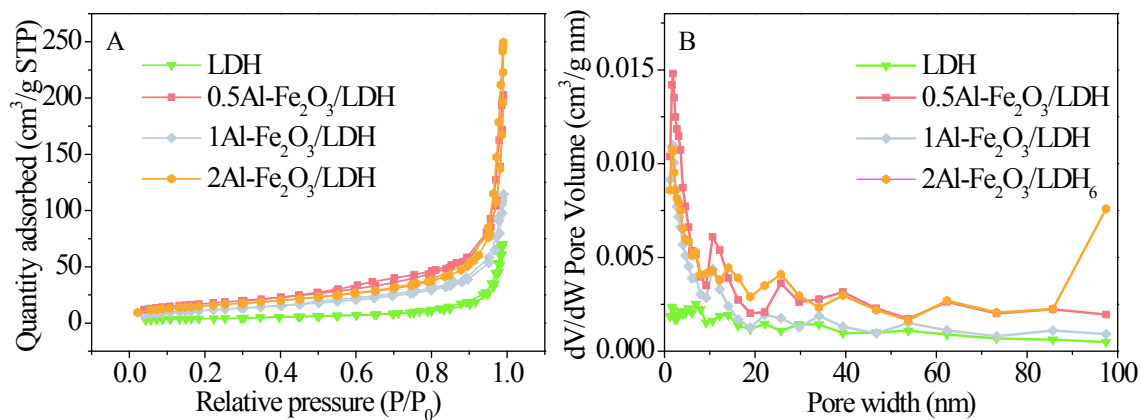


**Fig.S4.** Nitrogen removal/desorption analysis (A) and the pore size distribution (PSD)

curves of LDH, 0.5Al-Fe<sub>2</sub>O<sub>3</sub>/LDH, 1Al-Fe<sub>2</sub>O<sub>3</sub>/LDH ,and 2Al-Fe<sub>2</sub>O<sub>3</sub>/LDH.

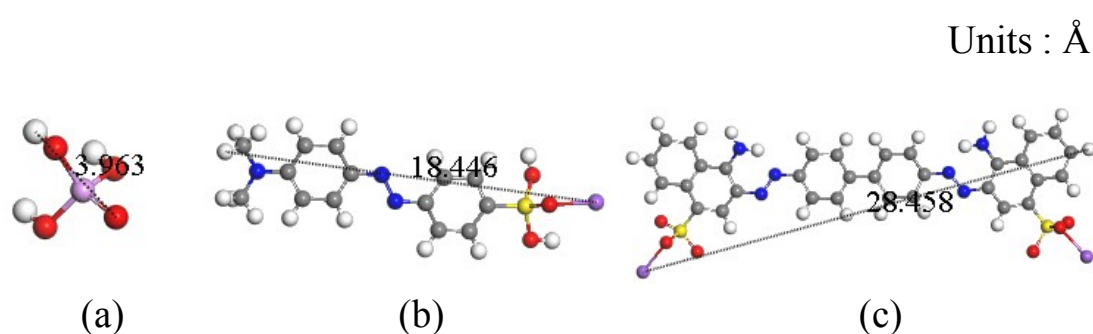


**Fig.S5.** The molecular size of phosphates (a), MO(b) and CR(c).

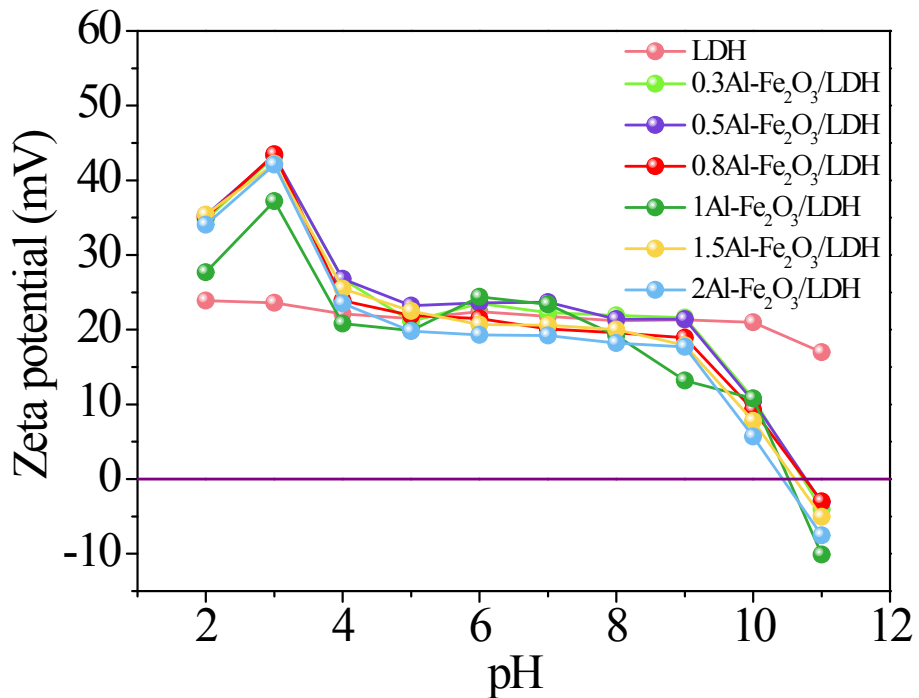


**Fig.S6.** Zeta potentials of LDH and Al- $\text{Fe}_2\text{O}_3$ /LDH assemblies as a function of pH.

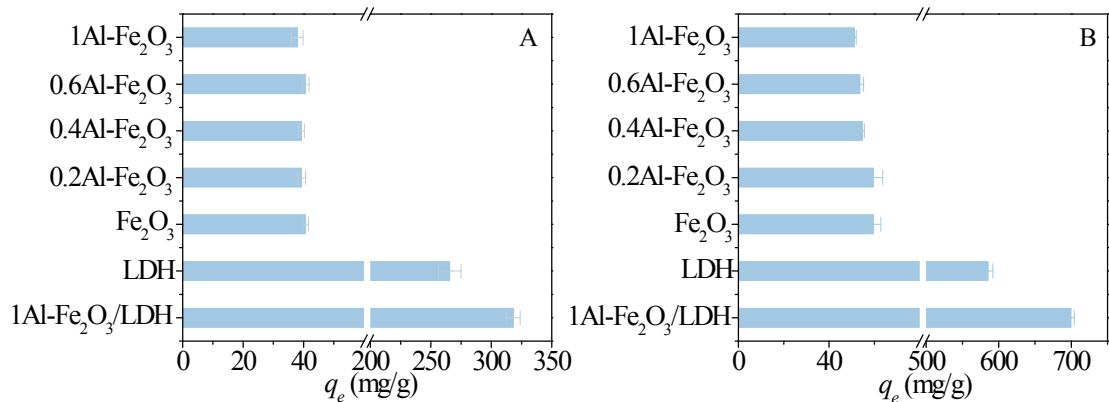


**Fig.S7.** Removal capacity of MO (A) and CR (B) on 1Al- $\text{Fe}_2\text{O}_3/\text{LDH}$ , LDH,  $\text{Fe}_2\text{O}_3$  and Al- $\text{Fe}_2\text{O}_3$  assemblies at  $\text{pH} = 5.5 \pm 0.1$ ,  $C_{\text{MO}} \text{ initial} = C_{\text{CR}} \text{ initial} = 200 \text{ mg/L}$ , 298K and  $m/V=0.2 \text{ g/L}$ .

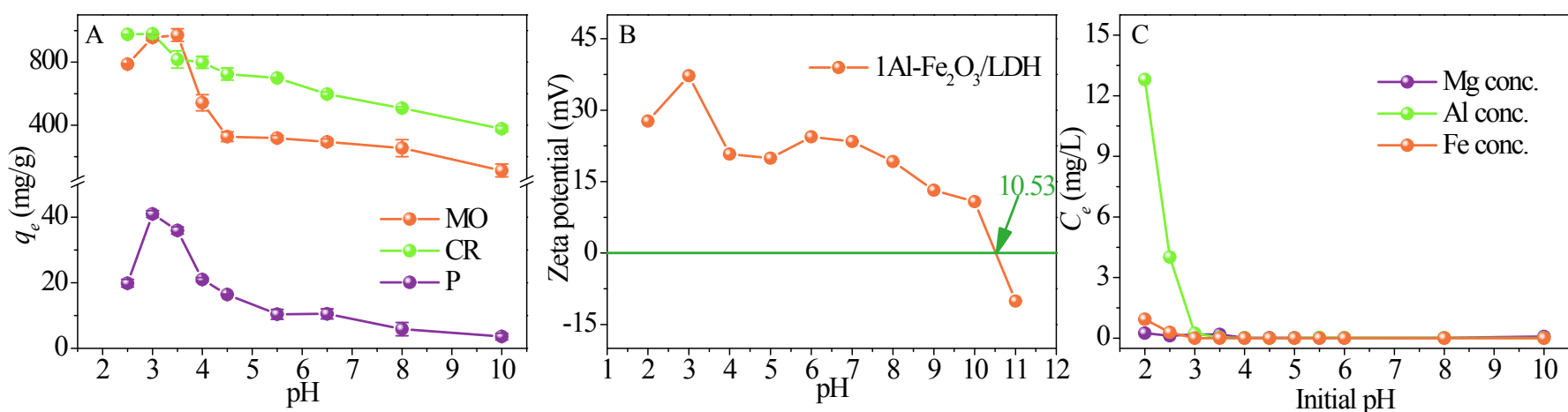


**Fig.S8.** Effect of initial pH on the removal of phosphates, MO and CR on the 1Al-Fe<sub>2</sub>O<sub>3</sub>/LDH,  $C_p$  initial = 10 mg/L,  $C_{MO}$  initial =  $C_{CR}$  initial = 200 mg/L, 298K and m/V=0.2 g/L (A) zeta potentials of 1Al-Fe<sub>2</sub>O<sub>3</sub>/LDH as a function of pH (B) the Mg, Al and Fe leaching at varying pH of 1Al-Fe<sub>2</sub>O<sub>3</sub>/LDH.

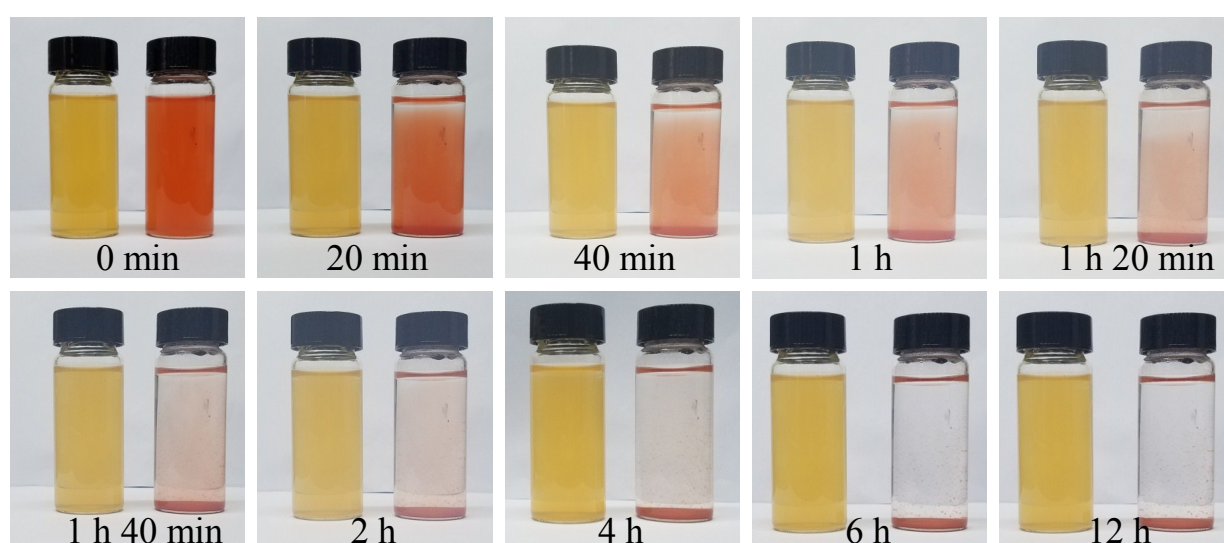


**Fig.S9.** The uniform dispersion before adsorption and the naturally settlement of 1Al-Fe<sub>2</sub>O<sub>3</sub>/LDH after adsorption.

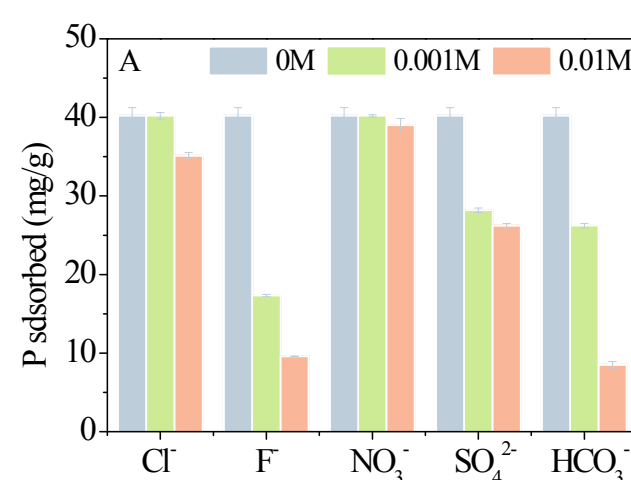


**Fig.S10.** Effects of coexisting ions on the phosphates adsorption capacity of 1Al-Fe<sub>2</sub>O<sub>3</sub>/LDH at different molar concentration, at 298K, m/V = 0.2 g/L, and  $C_p$  initial = 10 mg/L.

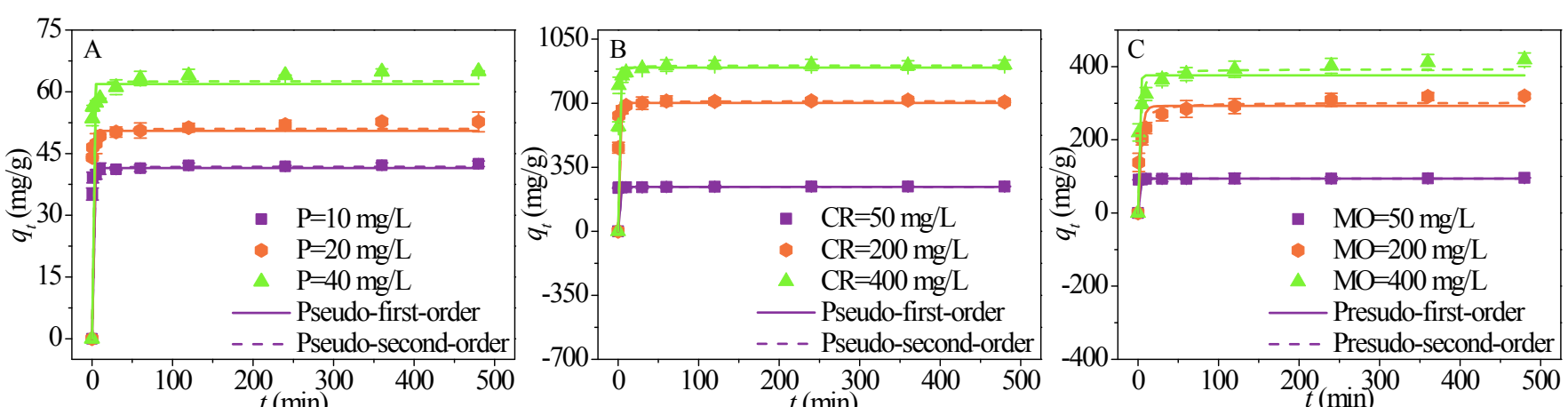


**Fig.S11.** The adsorption kinetics of phosphates (A), CR (B) and MO (C), at 298K, m/V = 0.2 g/L, and pH = 3 for phosphates and 5.5 for CR and MO.

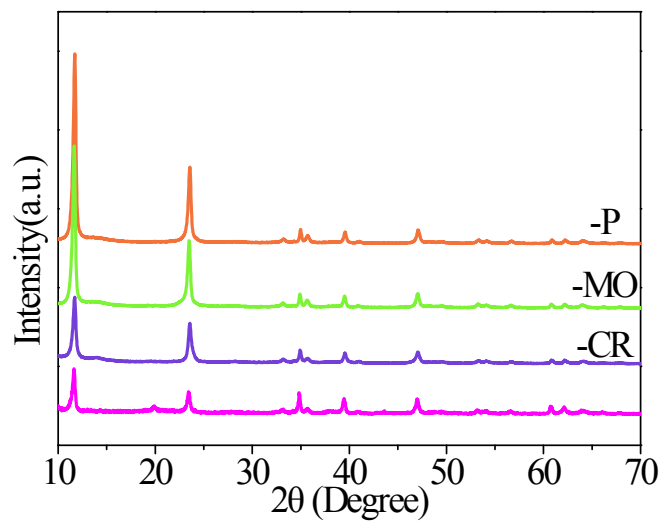


**Fig.S12.** XRD spectra of 1Al-Fe<sub>2</sub>O<sub>3</sub>/LDH before and after phosphates, MO and CR adsorption.

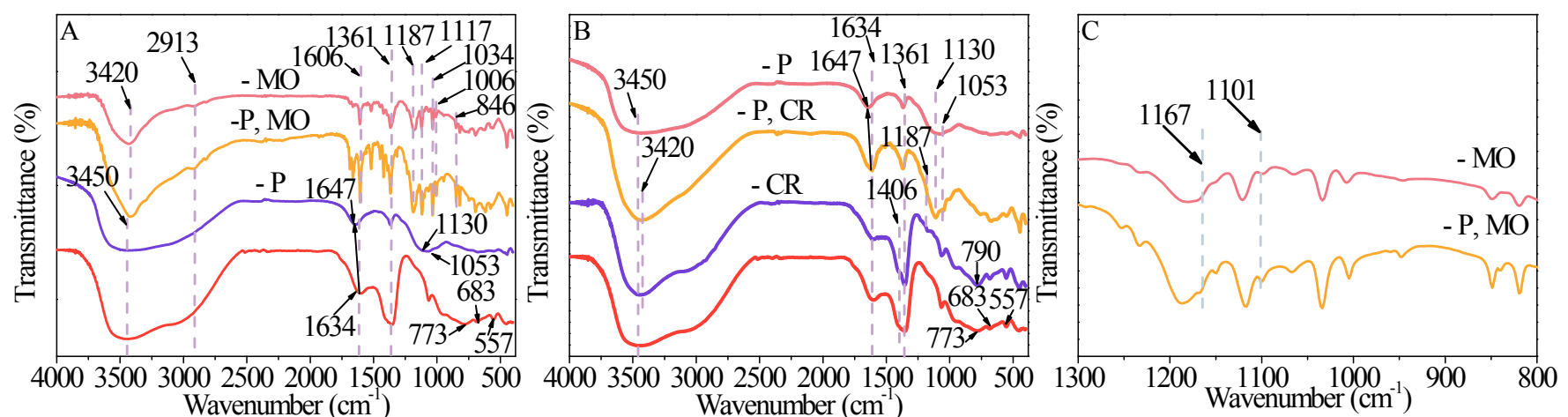


**Fig.S13.** FT-IR spectra of 1Al-Fe<sub>2</sub>O<sub>3</sub>/LDH before and after phosphates, MO and phosphates-MO (A); CR and phosphates-CR (B) adsorption; a magnification FT-IR spectra of A (C).

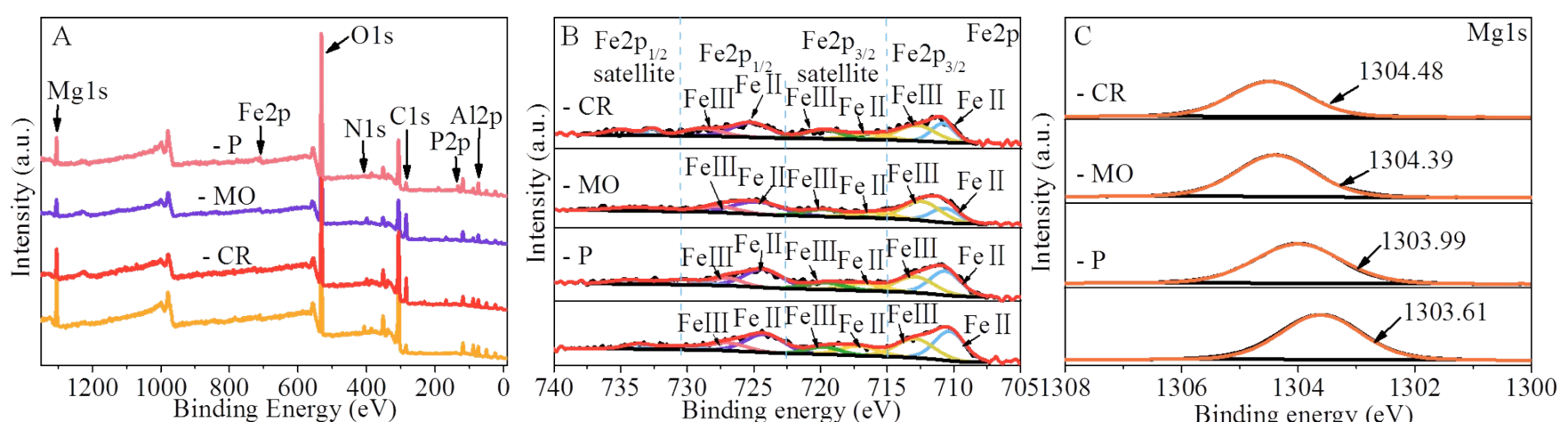


**Fig.S14.** Survey scan(A) and Fe2p (B) Mg1S (C) XPS spectra of 1Al-Fe<sub>2</sub>O<sub>3</sub>/LDH before and after adsorption of phosphates, MO and CR.

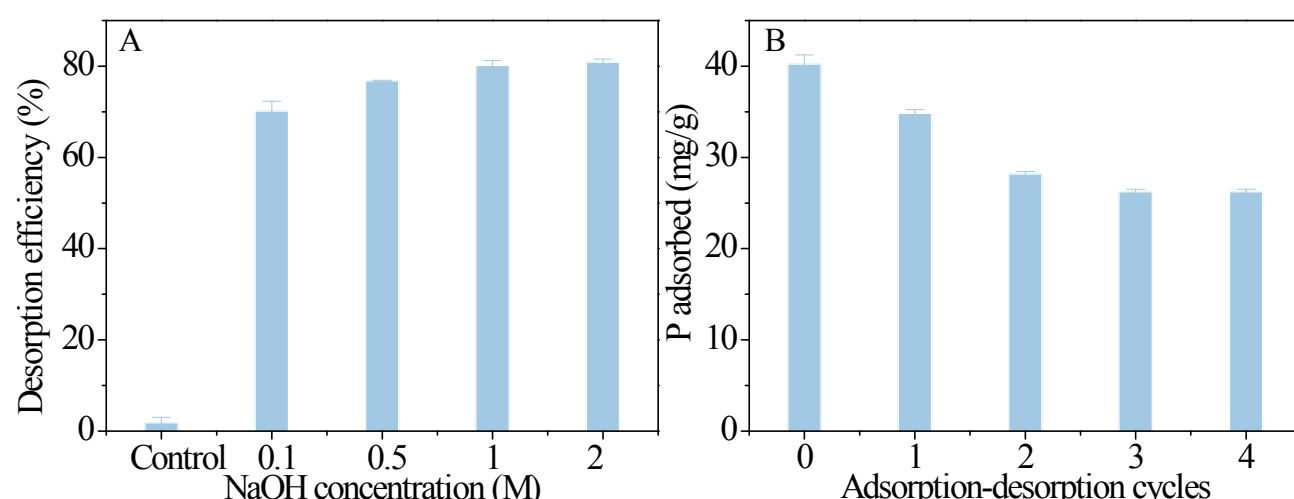


**Fig.S15.** Desorption efficiency at different NaOH concentrations(A) and adsorption–desorption cycles (B), at 298K,  $C_p$  initial = 10 mg/L and desorption time = 24 h.

**Table S1.** The actual ratio between Al and Fe in Al doped iron oxides materials.

	Fe <sub>2</sub> O <sub>3</sub>	0.2Al-Fe <sub>2</sub> O <sub>3</sub>	0.4Al-Fe <sub>2</sub> O <sub>3</sub>	0.6Al-Fe <sub>2</sub> O <sub>3</sub>	1Al-Fe <sub>2</sub> O <sub>3</sub>
Feeding ratio (Al:Fe)	0:1	0.2:1	0.4:1	0.6:1	1:1
Actual ratio (Al:Fe)	0:1	0.226:1	0.400:1	0.640:1	0.970:1

**Table S2.** Comparison of fitted kinetic model rate constants of phosphates and dyes (MO and CR) adsorption by different adsorbents.

Pollutants	Materials	Concentration (mg L <sup>-1</sup> )	pseudo-second-order rate constant (g mg <sup>-1</sup> min <sup>-1</sup> )			Reference	
Phosphates	1Al-Fe <sub>2</sub> O <sub>3</sub> /LDH	10, 20 and 40	0.29608	0.26804	0.16299	This work	
	MALZ	1, 5 and 10	0.048	0.023	0.013	<sup>1</sup>	
	CaT-Z	10 and 100	0.1158	0.0080		<sup>2</sup>	
	Mg/Al-LDHs biochar	50	0.0129			<sup>3</sup>	
	ACF-ZrFe	10, 20 and 30	0.00153	0.00054	0.00036	<sup>4</sup>	
	La-Uio-66	800	3.6 E-04			<sup>5</sup>	
	MO	1Al-Fe <sub>2</sub> O <sub>3</sub> /LDH	50,200 and 400	0.25563	0.00279	0.00223	This work
	MPL	100	1E-04			<sup>6</sup>	
	G-LDO	30	0.0015			<sup>7</sup>	
CR	1Al-Fe <sub>2</sub> O <sub>3</sub> /LDH	50,200 and 400	0.28714	0.00662	0.00464	This work	
	MPL	100	1E-04			<sup>6</sup>	
	Fe <sub>3</sub> O <sub>4</sub> /MgAlLDH	20	0.0187			<sup>8</sup>	

**Table S3.** Kinetic parameters for phosphate, CR and MO adsorption on 1Al-Fe<sub>2</sub>O<sub>3</sub>/LDH at different initial concentrations.

Adsorbates	C <sub>0</sub> (mg/L)	Pseudo first-order model			Pseudo second-order model			RMSE	
		q <sub>e</sub> (mg/g)	k <sub>1</sub> (min <sup>-1</sup> )	R <sup>2</sup>	q <sub>e</sub> (mg/g)	k <sub>2</sub> (g mg <sup>-1</sup> min <sup>-1</sup> )	R <sup>2</sup>		
phosphates	10	41.45467	3.64977	0.99548	0.83662	41.79279	0.29608	0.99765	0.60302
	20	48.15921	4.58835	0.97705	2.20772	51.65893	0.26804	0.99175	1.74545
	40	61.87574	3.7228	0.9745	2.99095	62.5786	0.16299	0.98467	2.31911
CR	50	242.87421	12.25561	0.99961	1.45053	243.01844	0.28714	0.99963	1.4082
	200	701.73305	2.16465	0.98854	21.54827	710.92586	0.00662	0.99001	15.96198
	400	894.476	2.10244	0.98686	27.28568	906.63197	0.00464	0.99018	20.98726
MO	50	97.27691	7.88806	0.99679	1.83949	96.8847	0.25563	0.99763	1.58313
	200	289.73277	0.63612	0.92815	28.57096	300.91474	0.00279	0.97027	18.37734
	400	385.0246	0.84609	0.95186	29.84901	394.56444	0.00223	0.97703	20.61977

**Table S4.** Adsorption equilibrium models and parameters for removal of P,CR and MO.

Parameters	P			CR			MO		
	288K	298K	308K	288K	298K	308K	288K	298K	308K
Experiment result (mg/g)	63.22169	72.30443	78.30196	1027.7825	1042.55768	1062.5173	349.88632	417.85857	541.19365
<b>Langmuir</b>									
q <sub>m</sub> (mg/g)	59.30695	66.20219	71.27827	919.05663	920.19867	921.66961	479.34932	577.42028	849.98858
K <sub>L</sub> (L/mg)	1.14346	1.30388	1.58778	0.08388	0.11902	0.29188	7.58015E-03	8.41236E-03	6.15394E-03
R <sup>2</sup>	0.9266	0.91092	0.92474	0.9052	0.91138	0.91793	0.97554	0.98541	0.98697
<b>Freundlich</b>									
K <sub>F</sub> (mg <sup>1-1/n</sup> L <sup>1/n</sup> g <sup>-1</sup> )	31.41602	35.49254	39.60522	195.2576	223.53304	299.11051	17.87385	23.24246	20.76887
1/n	0.20489	0.20819	0.19485	0.28971	0.26977	0.22418	0.51721	0.51116	0.58290
R <sup>2</sup>	0.94816	0.95064	0.95630	0.94634	0.93886	0.92394	0.95132	0.94616	0.96405
<b>Langmuir-Freundlich</b>									
K <sub>LF</sub> (mg <sup>1-1/n</sup> L <sup>1/n</sup> g <sup>-1</sup> )	50.46097	56.84887	70.83681	169.63446	198.96806	321.44441	3.33311	2.40970	3.33179
a <sub>LF</sub> (mg <sup>-1/n</sup> L <sup>1/n</sup> )	0.64426	0.61089	0.75561	0.11009	0.14592	0.27209	0.0071	0.00475	0.00442
1/n	0.49881	0.46122	0.47143	0.48269	0.50525	0.52322	1.02323	1.18837	1.12047
R <sup>2</sup>	0.97220	0.96681	0.97686	0.94931	0.94728	0.94784	0.96948	0.98497	0.98492

**Table S5.** Comparison of fitted equilibrium model capacity of phosphates and dyes (MO and CR) adsorption by different adsorbents.

Materials	Phosphates (mg g-1)	MO (mg g-1)	CR (mg g-1)	Reference
1Al-Fe2O3/LDH	93.06	577.42	1363.54	This work
MPL		624.89	584.56	6
Ni/Al LDH decorated PAB		412.8		9
NMA-LDOs			1250	10
MALZ	80.8			1
MFC@La(OH) <sub>3</sub>	45.45			11

**Table S6.** Values of thermodynamic parameters for P, CR and MO adsorption.

Temperature(K)	P			MO			CR		
	$\Delta G^0$ (kJ/mol)	$\Delta S^0$ (J/(mol K))	$\Delta H^0$ (kJ/mol)	$\Delta G^0$ (kJ/mol)	$\Delta S^0$ (J/(mol K))	$\Delta H^0$ (kJ/mol)	$\Delta G^0$ (kJ/mol)	$\Delta S^0$ (J/(mol K))	$\Delta H^0$ (kJ/mol)
288	-9.485	130.610	28.158	-3.559	53.762	11.927	-10.550	128.454	26.453
298	-10.703			-4.088			-11.808		
308	-12.102			-4.635			-12.121		

**Table S7.** Adsorption equilibrium models and parameters for removal of P with different CR concentrations.

Parameters	P+0CR	P+50CR	P+100CR	P+200CR
	298K	298K	298K	298K
<b>Experiment result (mg/g)</b>	72.30443	50.25153	41.79794	37.32985
<b>Langmuir</b>				
$q_m$ (mg/g)	66.20219	50.00320	39.92727	36.54688
$K_L$ (L/mg)	1.30388	0.69553	0.54643	0.53266
$R^2$	0.91092	0.8366	0.77626	0.78197
<b>Freundlich</b>				
$K_F$ ( $\text{mg}^{1-1/n}\text{L}^{1/n}\text{g}^{-1}$ )	35.49254	24.14363	19.07382	17.54690
$1/n$	0.20819	0.22588	0.23126	0.21665
$R^2$	0.95064	0.98098	0.98284	0.98918
<b>Langmuir-Freundlich</b>				
$K_{LF}$ ( $\text{mg}^{1-1/n}\text{L}^{1/n}\text{g}^{-1}$ )	56.84887	27.61392	19.19071	17.75060
$a_{LF}$ ( $\text{mg}^{-1/n}\text{L}^{1/n}$ )	0.61089	0.16038	0.00748	0.01311
$1/n$	0.46122	0.28952	0.23411	0.22136
$R^2$	0.96681	0.97887	0.9791	0.98671

**Table S8.** Adsorption equilibrium models and parameters for removal of P with different MO concentrations.

Parameters	P+0MO	P+50MO	P+100MO	P+200MO
	298K	298K	298K	298K
<b>Experiment result (mg/g)</b>	72.30443	63.44245	61.31592	59.79548
<b>Langmuir</b>				
$q_m$ (mg/g)	66.20219	61.15062	59.75222	59.58753
$K_L$ (L/mg)	1.30388	0.75369	0.61536	0.45025
$R^2$	0.91092	0.95281	0.97809	0.97601
<b>Freundlich</b>				
$K_F$ ( $\text{mg}^{1-1/n}\text{L}^{1/n}\text{g}^{-1}$ )	35.49254	30.63096	28.3496	25.66921
$1/n$	0.20819	0.2093	0.22097	0.2402
$R^2$	0.95064	0.87916	0.91043	0.90391
<b>Langmuir-Freundlich</b>				
$K_{LF}$ ( $\text{mg}^{1-1/n}\text{L}^{1/n}\text{g}^{-1}$ )	56.84888	46.19470	38.39131	28.41539
$a_{LF}$ ( $\text{mg}^{-1/n}\text{L}^{1/n}$ )	0.61089	0.72344	0.59657	0.45912
$1/n$	0.46122	0.85	0.7862	0.88679
$R^2$	0.96681	0.94644	0.97422	0.97337

**Table S9.** Adsorption equilibrium models and parameters for removal of CR with different P concentrations.

Parameters	CR+0P	CR+10P	CR+20P
	298K	298K	298K
<b>Experiment result (mg/g)</b>	1042.55768	994.92331	967.04371
<b>Langmuir</b>			
$q_m$ (mg/g)	920.19867	963.37159	905.79401
$K_L$ (L/mg)	0.11902	0.04046	0.04535
$R^2$	0.91138	0.94914	0.92867
<b>Freundlich</b>			
$K_F$ (mg <sup>1-1/n</sup> L <sup>1/n</sup> g <sup>-1</sup> )	223.53304	144.95529	145.45645
$1/n$	0.26977	0.33706	0.32713
$R^2$	0.93886	0.96000	0.94801
<b>Langmuir-Freundlich</b>			
$K_{LF}$ (mg <sup>1-1/n</sup> L <sup>1/n</sup> g <sup>-1</sup> )	198.96806	98.75088	107.08916
$a_{LF}$ (mg <sup>-1/n</sup> L <sup>1/n</sup> )	0.14592	0.07080	0.07644
$1/n$	0.50525	0.59430	0.55467
$R^2$	0.94728	0.96927	0.95085

**Table S10.** Adsorption equilibrium models and parameters for removal of MO with different P concentrations.

Parameters	MO+0P	MO+10P	MO+20P
	298K	298K	298K
<b>Experiment result (mg/g)</b>	417.85857	405.31123	393.68057
<b>Langmuir</b>			
$q_m$ (mg/g)	577.42028	686.77207	735.43108
$K_L$ (L/mg)	8.41236E-03	4.62123E-03	3.67414E-03
$R^2$	0.98541	0.97752	0.98103
<b>Freundlich</b>			
$K_F$ (mg <sup>1-1/n</sup> L <sup>1/n</sup> g <sup>-1</sup> )	23.24246	10.78785	8.30451
$1/n$	0.51116	0.63792	0.67677
$R^2$	0.94616	0.94137	0.95340
<b>Langmuir-Freundlich</b>			
$K_{LF}$ (mg <sup>1-1/n</sup> L <sup>1/n</sup> g <sup>-1</sup> )	2.40970	0.34738	0.31805
$a_{LF}$ (mg <sup>-1/n</sup> L <sup>1/n</sup> )	0.00475	7.58030E-04	6.79245E-04
$1/n$	1.18837	1.56030	1.53010
$R^2$	0.98497	0.99311	0.99342

**Table S11.** Binding energies of elements in 1Al-Fe<sub>2</sub>O<sub>3</sub>/LDH before adsorption and after pollutants adsorption.

	<i>E<sub>B</sub>(eV)</i>				
	C1s	O1s	Mg1s	Al2p	Fe2p
1Al-Fe <sub>2</sub> O <sub>3</sub> /LDH	284.8	531.90	1303.61	74.03	710.75
1Al-Fe <sub>2</sub> O <sub>3</sub> /LDH-MO	284.8	532.00	1304.39	74.31	711.59
1Al-Fe <sub>2</sub> O <sub>3</sub> /LDH-CR	284.8	532.32	1304.48	74.67	711.44
1Al-Fe <sub>2</sub> O <sub>3</sub> /LDH-P	284.8	531.73	1303.99	74.14	711.31
					133.49

**Table S12.** Binding energies of Fe2p in 1Al-Fe<sub>2</sub>O<sub>3</sub>/LDH before adsorption and after pollutants adsorption.

	<i>E<sub>B</sub>(eV)</i>								
	Fe2p <sub>1/2</sub> satellite			Fe2p <sub>1/2</sub>		Fe2p <sub>3/2</sub> satellite		Fe2p <sub>3/2</sub>	
	Fe III	Fe II	Fe III	Fe II	Fe III	Fe II	Fe III	Fe II	
1Al-Fe <sub>2</sub> O <sub>3</sub> /LDH	733.72	730.70	727.05	724.17	719.75	717.17	712.89	710.31	
1Al-Fe <sub>2</sub> O <sub>3</sub> /LDH-MO	735.03	732.26	727.71	724.83	719.85	716.03	712.51	710.76	
1Al-Fe <sub>2</sub> O <sub>3</sub> /LDH-CR	735.03	732.69	728.95	725.30	719.89	716.50	712.88	710.93	
1Al-Fe <sub>2</sub> O <sub>3</sub> /LDH-P	734.42	730.42	727.05	724.36	719.72	716.75	712.94	710.69	

## Reference

1. W. Shi, Y. Fu, W. Jiang, Y. Ye, J. Kang, D. Liu, Y. Ren, D. Li, C. Luo and Z. Xu, Enhanced phosphate removal by zeolite loaded with Mg–Al–La ternary (hydr)oxides from aqueous solutions: Performance and mechanism, *Chem. Eng. J.*, 2019, **357**, 33-44.
2. D. Mitrogiannis, M. Psychoyou, I. Baziotis, V. J. Inglezakis, N. Koukouzas, N. Tsoukalas, D. Palles, E. Kamitsos, G. Oikonomou and G. Markou, Removal of phosphate from aqueous solutions by adsorption onto Ca(OH)<sub>2</sub> treated natural clinoptilolite, *Chem. Eng. J.*, 2017, **320**, 510-522.
3. R. Li, J. J. Wang, B. Zhou, M. K. Awasthi, A. Ali, Z. Zhang, L. A. Gaston, A. H. Lahori and A. Mahar, Enhancing phosphate adsorption by Mg/Al layered double hydroxide functionalized biochar with different Mg/Al ratios, *Sci. Total. Environ.*, 2016, **559**, 121-129.
4. W. Xiong, J. Tong, Z. Yang, G. Zeng, Y. Zhou, D. Wang, P. Song, R. Xu, C. Zhang and M. Cheng, Adsorption of phosphate from aqueous solution using iron-zirconium modified activated carbon nanofiber: Performance and mechanism, *J. Colloid Interface Sci.*, 2017, **493**, 17-23.
5. X. Min, X. Wu, P. Shao, Z. Ren, L. Ding and X. Luo, Ultra-high capacity of lanthanum-doped UiO-66 for phosphate capture: Unusual doping of lanthanum by the reduction of coordination number, *Chem. Eng. J.*, 2019, **358**, 321-330.
6. J. Li, Q. Fan, Y. Wu, X. Wang, C. Chen, Z. Tang and X. Wang, Magnetic polydopamine decorated with Mg–Al LDH nanoflakes as a novel bio-based adsorbent for simultaneous removal of potentially toxic metals and anionic dyes, *J. Mater. Chem.*, 2016, **4**, 1737-1746.
7. W. Yao, S. Yu, J. Wang, Y. Zou, S. Lu, Y. Ai, N. S. Alharbi, A. Alsaedi, T. Hayat and X. Wang, Enhanced removal of methyl orange on calcined glycerol-modified nanocrystalline Mg/Al layered double hydroxides, *Chem. Eng. J.*, 2017, **307**, 476-486.
8. R.-r. Shan, L.-g. Yan, K. Yang, S.-j. Yu, Y.-f. Hao, H.-q. Yu and B. Du, Magnetic Fe<sub>3</sub>O<sub>4</sub>/MgAl-LDH composite for effective removal of three red dyes from aqueous solution, *Chem. Eng. J.*, 2014, **252**, 38-46.
9. S. Chen, Y. Huang, X. Han, Z. Wu, C. Lai, J. Wang, Q. Deng, Z. Zeng and S. Deng, Simultaneous and efficient removal of Cr(VI) and methyl orange on LDHs decorated porous carbons, *Chem. Eng. J.*, 2018, **352**, 306-315.
10. C. Lei, X. Zhu, B. Zhu, C. Jiang, Y. Le and J. Yu, Superb adsorption capacity of hierarchical calcined Ni/Mg/Al layered double hydroxides for Congo red and Cr(VI) ions, *J. Hazard. Mater.*, 2017, **321**, 801-811.
11. T. Liu, X. Chen, X. Wang, S. Zheng and L. Yang, Highly effective wastewater phosphorus removal by phosphorus accumulating organism combined with magnetic sorbent MFC@La(OH)3, *Chem. Eng. J.*, 2018, **335**, 443-449.